

# Techniques of differential scanning calorimetry for quantification of low contents of amorphous phases

Minna Lappalainen · Maarit Karppinen

Received: 9 March 2010 / Accepted: 15 April 2010 / Published online: 23 June 2010  
© Akadémiai Kiadó, Budapest, Hungary 2010

**Abstract** Differential scanning calorimetry (DSC) is one of the most frequently used techniques for analyzing small concentrations of amorphous phases in a crystalline matrix. In recent years novel enhanced DSC approaches have been intensively looked for to improve parameters such as sensitivity, accuracy, and detection limit of the technique. Low levels of amorphous phases can be quantitatively determined in DSC by measuring the heat capacity change associated with the glass transition. In this short review the potentials provided by the HyperDSC and StepScan DSC techniques are discussed. Examples illustrate the advantages and disadvantages of the techniques and compare their abilities to detect small glass transitions and determine low contents of amorphous phases in samples which are mostly crystalline.

**Keywords** Thermal analysis · Differential scanning calorimetry · HyperDSC · StepScan DSC · Amorphous content · Glass transition

## Introduction

The degree of crystallinity is an important parameter for various food and pharmaceutical systems as it affects their behavior during processing, storage, and consumption. Presence of even a tiny amount of amorphous component(s) in a crystalline product may have considerable impact on the stability, processability, and bioavailability

of the material and its performance during product manufacture and use [1–3]. It is, therefore, of great importance to search for means to assess the extent of disorder in a solid quantitatively, down to very low concentration levels.

The amorphous phases in materials such as sugars and pharmaceuticals are typically formed unintentionally, and the challenge arises from the fact that the concentration of disordered material is often high enough to cause changes in product performance but yet too small to be easily detected [4–6]. A number of techniques are available for the detection and quantification of low levels of amorphous components, but the methods are usually sample-specific. There are several studies reported in the literature where different techniques for determination of the content of amorphous phase(s) are compared as analysis methods [5–10]. Each technique has its own advantages and disadvantages. The method of choice depends for example on the concentration level of the amorphous phase and the amount of sample available. In addition, there are differences in the sample preparation procedure and the time required by the measurement. Table 1 summarizes the various techniques employed.

Differential scanning calorimetry (DSC) is one of the most frequently used techniques for the measurement of the degree of amorphicity. Owing to difficulties in detection of very low concentrations of amorphous phases by means of the conventional DSC technique, in recent years novel DSC approaches have been intensively looked for to improve parameters such as sensitivity, accuracy, and detection limit. The high-speed or high-performance differential scanning calorimetry (HyperDSC) technique, in which an increased heating rate is used, significantly improves the sensitivity of DSC as it allows small transitions to be detected more readily [11–26]. Moreover, several versions of another approach have been proposed

---

M. Lappalainen · M. Karppinen (✉)  
Laboratory of Inorganic Chemistry, Department of Chemistry,  
Aalto University School of Science and Technology, 00076  
Aalto, Finland  
e-mail: maarit.karppinen@tkk.fi

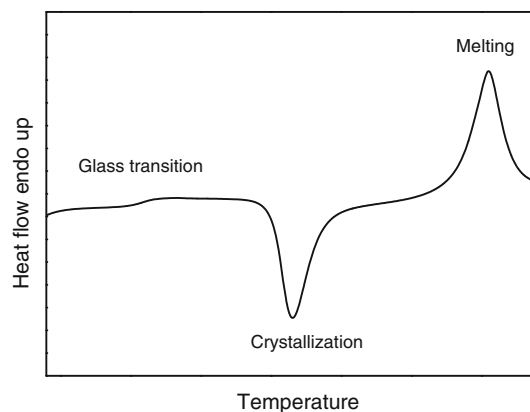
**Table 1** Analytical methods employed and their detection limits for quantification of amorphous phases

| Method  | Detection limit/% | References       |
|---|-------------------|------------------|
| X-ray powder diffraction (XRD)                  | 0.4–10            | [57–61]          |
| Differential scanning calorimetry (DSC)         | 1–20              | [60–63]          |
| High-speed DSC (HyperDSC)                       | 0.2–1.5           | [15–19]          |
| StepScan DSC                                    | 0.8               | [8, 44]          |
| Temperature-modulated DSC (TMDSC)               | 0.9               | [17, 64, 65]     |
| Gravimetric moisture sorption (GMS)             | 0.5–1             | [66, 67]         |
| Solution calorimetry (SC)                       | 0.5–1.8           | [68–70]          |
| Isothermal microcalorimetry (IMC)               | 0.5–5             | [61, 67, 68, 71] |
| Dynamic mechanical analysis (DMA)               | 2                 | [72]             |
| Density measurements                            | 10                | [5]              |
| Solid-state nuclear magnetic resonance (SS-NMR) | 0.5–3             | [57, 63, 71]     |
| Fourier transform infrared spectroscopy (FTIR)  | 1–2               | [9, 73]          |
| Raman spectroscopy                              | 1                 | [74, 75]         |
| Near infrared spectroscopy (NIR)                | 0.5–1             | [59, 66]         |
| Thermally stimulated current spectrometry       | ~1                | [76]             |
| Inverse phase gas chromatography                | 1                 | [77, 78]         |

including the temperature-modulated DSC (TMDSC) [27–39], TOPEM (advanced temperature-modulated DSC) [40–43], and StepScan DSC [44–56] techniques. These techniques allow for reversible changes to be distinguished from the potentially interfering irreversible kinetic events by way of temperature modulation. In this short review we discuss the abilities of the HyperDSC and StepScan DSC techniques to detect and quantify low contents of amorphous phases in samples which are mostly crystalline. In the earlier reviews dealing with the determination of amorphicity in general, the DSC methods have not been extensively discussed.

### Glass transition seen by differential scanning calorimetry

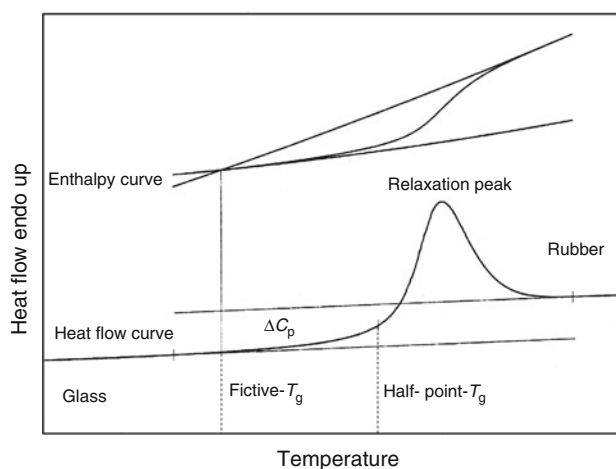
A typical DSC scan for a totally or partially amorphous sample is shown in Fig. 1; the curve displays a glass transition, a crystallization exotherm, and a melting endotherm [79]. The glass transition is seen as a change in heat capacity ( $C_p$ ) on heating. The magnitude of  $\Delta C_p$  at glass transition temperature ( $T_g$ ) varies from compound to compound, and this variance is the basis for the classification of glass formers to strong and fragile glass formers [80]. Above  $T_g$  the sample viscosity gradually decreases with increasing temperature such that at some point (crystallization temperature) the molecules gain enough freedom to spontaneously arrange

**Fig. 1** Schematic DSC curve for a non-annealed amorphous sample upon heating

themselves into a form of crystalline solid. This first-order transition appears as an exothermic peak in the DSC curve. Finally upon further heating the sample melts. This gives an endothermic signal in the DSC data.

A special problem related to DSC studies dealing with the glass transition is caused by the fact that an amorphous system carries a memory of its thermal history. Different cooling rates result in glasses of different degrees of order. Note that the glassy solid is thermodynamically far from equilibrium, and only the liquid or rubber state is at thermodynamic equilibrium. Glasses are known to change their properties when annealed at temperatures below their  $T_g$  [81–87]. The structure of a non-annealed glass is close to the structure of the corresponding liquid, and accordingly,  $\Delta C_p$  at  $T_g$  is smaller for a non-annealed than an annealed glass [88].

The glass transition is a second-order transition and it is seen in the DCS data as a step in the baseline in the heat flow versus temperature curve (Figs. 1, 2). The

**Fig. 2** Glass transition seen in the DSC data, in the heat flow curve, and in the enthalpy curve

endothermic peak often observed on the heat flow curve at the end of the glass transition range (Fig. 2) is known as the enthalpy relaxation peak; it is the recovery of the enthalpy lost during the annealing process below the  $T_g$  and it corresponds to the enthalpy difference between an annealed glass and a quenched (non-annealed) glass [79, 84, 85]. The relaxation peak may also arise if the heating and cooling rates are different. When a slowly cooled material is heated with a faster rate over the glass transition than was the case on cooling, rapid heating does not allow sufficient time for molecules to relax at the glass transition and extra energy at a higher temperature is needed for relaxation of molecules to the rubber state [4, 89]. The presence of a relaxation endotherm may complicate the determination of  $T_g$  because the baseline shift may sometimes render the identification and quantification of the glass transition extremely difficult.

As already mentioned above, the glass transition is a dynamic (not thermodynamical) phenomenon. Accordingly, the  $T_g$  depends not only on the thermal history of the sample but also on the temperature scanning rate [90–92]. It should also be noted that the glass transition temperatures are extremely sensitive to water. The residual moisture in material acts as a plasticizer by increasing the free volume of the material. Hence, it has a profound influence on the glass transition of amorphous materials leading to a decrease in  $T_g$  [4, 89, 93–97].

There are at least three ways to determine the value of  $T_g$  from the DSC data. The so-called “half-point- $T_g$ ” is the temperature that corresponds to the point on the heat flow curve where  $\Delta C_p$  reaches 50% of the total change in the specific heat capacity about the transition. At half-point- $T_g$  the heat capacity is midway between those of the glassy and the liquid states. The  $T_g$  may also be read at the inflection point of the DSC curve associated with the glass transition. However, in case a large relaxation peak follows the glass transition, the inflection point revealed from the curve is often displaced from the real inflection point of the glass transition [88]. This is why the inflection point is seldom used to define the value of  $T_g$  [79]. The third way to determine the value of  $T_g$  is to find the intersection of the extrapolated pre-transition and post-transition baselines on the enthalpy curve that is the integral of the specific heat curve [4, 98], see Fig. 2. This point is called “fictive- $T_g$ ” (i.e., “thermodynamic” or “enthalpic” glass transition temperature) [79].

### Quantitative analysis of amorphous content by differential scanning calorimetry

Traditionally the exothermic crystallization peak which follows—upon heating—the glass transition has been used

for quantitative analysis of the content of amorphous phase(s) [5, 59–61, 99]. In some studies (in case no crystallization occurs) even the melting enthalpy has been used for quantifying the degree of amorphicity [57, 62]. However, it is difficult to quantify particularly the small concentration of the amorphous phase with confidence in these techniques. It is hence preferable to use the glass transition for the quantification of the amorphous content. With appropriate calibration, the magnitude of  $\Delta C_p$  at  $T_g$  and thereby the amorphous content may be determined in a highly quantitative way. Note that  $\Delta C_p$  is linearly proportional to the amorphous content provided that the amorphous glasses are in the same state both in the actual sample studied and in the reference samples used for calibration [38]. Great care is, however, required if the change in the  $C_p$  value at  $T_g$  is to be measured quantitatively. To obtain reliable results, it is essential to perform a calibration using a standard such as sapphire [4]. Moreover, baseline calibration is needed to ensure as flat baseline as possible.

Quantitative determination of amorphous phases requires 100% pure crystalline and amorphous standards as well as well-defined samples with various degrees of crystallinity for reference. A commonly accepted technique to prepare a standard series of samples with various known degrees of crystallinity is to simply weigh and thoroughly mix fully amorphous and fully crystalline samples at various ratios. A check for homogeneity of such a mixture can be done by observing the standard deviation of several measurements performed with the same mixture [7]. However, preparation of samples with various degrees of crystallinity (in average) by mixing the fully amorphous and fully crystalline samples produces mixtures in which the crystalline and amorphous portions exist separately in different particles [1, 5, 8]. This does not perfectly correspond to the real situation where amorphous and crystalline portions are normally in intimate contact with each other in each individual particle.

A starting point in the development of a method for the determination of amorphous content is to ensure that the  $\Delta C_p$  value for a 100% amorphous sample can be determined in a reproducible manner. Here the first step is to find the proper annealing temperature and time for the reference sample to eliminate the effect of thermal history of the sample and thereby reach a constant  $\Delta C_p$  value. After the proper annealing conditions have been found, an appropriate temperature program can be made. This program is then used for the measurements of the fully crystalline and the fully amorphous samples as well as the synthetic mixtures. From the results, the  $\Delta C_p$  value at the  $T_g$  as a function of the degree of amorphicity can be found and a linear regression line can be calculated.

## Novel enhanced DSC techniques

There are two new DSC approaches that have already been shown to greatly improve the detection of the glass transition. In the HyperDSC technique a high heating rate is used to allow small transitions to be detected more readily [11–26], whereas in the TMDSC techniques the heating program is modulated such that the reversible changes in specific heat capacity may be distinguished from potentially interfering irreversible kinetic events such as the enthalpy relaxation. In the TMDSC technique, using conventional heat-flux DSC equipment, periodic temperature oscillations are applied to the system. The heating-block temperature is sinusoidally modulated such that the sample temperature is modulated in the same manner about a constant period. The modulated temperature and the resultant modulated heat flow are then typically deconvoluted using a Fourier transform to obtain the reversible and non-reversible components [27–39]. The StepScan DSC method, on the other hand, employs a high-sensitive power-compensated DSC equipment. The sample follows a heat-hold temperature program, and the program allows equilibration of the system after each step in a series of small step-wise increases in temperature. As a result the reversible and non-reversible components are obtained without mathematical operations [44–56]. In the following, the HyperDSC and StepScan DSC techniques are discussed in more detail.

### HyperDSC

The HyperDSC technique is based on a relatively new technology but has already attracted considerable interest as a method of high sensitivity. The technique employs very fast heating and cooling rates of up to  $500\text{ }^{\circ}\text{C min}^{-1}$ , and requires an instrument with an extremely fast response time with respect to the chosen temperature program together with a very high resolution. This can only be achieved using a power-compensated DSC apparatus in which the low furnace mass and small dimensions ensure much faster heat transfer compared to the situation with the heat-flux DSCs [11–14]. The high heating rate significantly increases the sensitivity because an increased scan rate leads to a higher heat flow. The DSC output is measured as a function of heat flow (mW), which can also be expressed as energy per unit time (J/s). At fast scan rates, the same amount of heat flows over a shorter time period. Therefore, the use of increased heating rates allows extremely small transitions that would be below the limit of detection at the heating rates employed in conventional DSC to be measured. The HyperDSC technique also allows the measurement of much smaller samples [11, 12, 15–17, 20, 21], and has over the last few years found a variety of applications

in the fields of pharmaceuticals and polymers ranging from studies of polymorphism and glass transitions to those of the kinetics of macromolecular and pharmaceutical systems [12–26].

Higher scanning rates also aid the visualization of the  $T_g$  in samples with only a small amount of the amorphous phase embedded in crystalline matrix [4, 16, 17, 21]. Hence HyperDSC should be considered as a highly plausible technique for studying glass transitions. The technique can offer a huge improvement in sensitivity and speed over the conventional and modulated DSC techniques [11, 17], and is able to provide us with valuable information rapidly and on small samples, opening a new area for research on amorphous materials [15].

There are, however, some limitations to the technique. Resolution is one of the concerns to be addressed [17]. At high heating rates, thermal gradients within the sample may have an impact, widening the signals detected from the glass transition and other thermal events and superimposing these phenomena inside the material. One way to reduce the thermal gradient is to use samples of very small masses. On the other hand, a certain minimum mass is needed to ensure an acceptable signal-to-noise ratio and a measurable signal. Hence, a compromise has to be found [12]. To achieve optimal thermal contact between the sample and the sample container, aluminum foil or a thin-foil sample pan may be used [12, 14, 25]. Corrections concerning thermal lag are often found to be necessary and have been used and discussed [25, 26].

Both Saunders et al. [15] and Gabbott et al. [16] have evaluated the potential of the HyperDSC technique to characterize low amorphous contents in lactose samples. Different heating rates were tested, and the linear control of the heating rate for all the high scan rates used ( $50\text{--}500\text{ }^{\circ}\text{C min}^{-1}$ ) was demonstrated. The size of the DSC response increased substantially as the scan rate was increased, and it became easier to detect the glass transition even for samples with  $\sim 1\%$  amorphicity when using very low sample masses. Mixtures of crystalline and amorphous (spray dried) lactose were prepared, and the heating rate of  $500\text{ }^{\circ}\text{C min}^{-1}$  was chosen for the measurements because this rate was found to show the largest glass transition on the spray-dried lactose. The step height change of the glass transition was measured from the onset to the maximum height for each sample, and a linear relationship between this value and amorphicity was found [15, 16]. An independent sample that had been found to contain  $1\%$  amorphicity by a solution calorimetry method was measured under the same conditions, a clear glass transition was seen which well verified the sensitivity of the HyperDSC technique [16].

The sensitivity of HyperDSC has also been tested for various maltitol samples. Even for a sample with  $1\%$

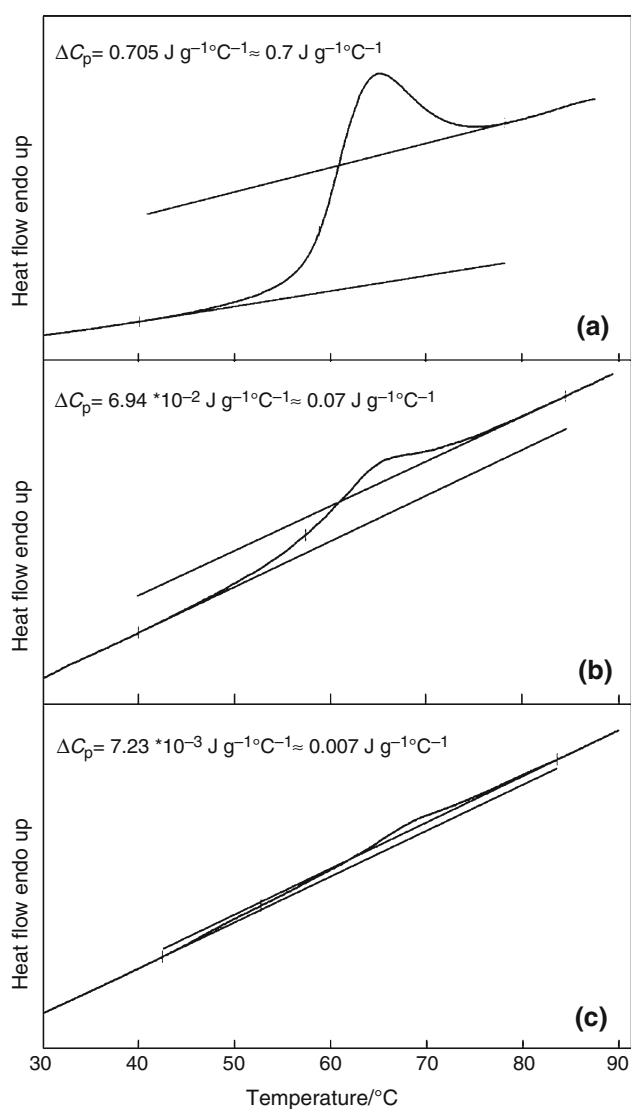


**Fig. 3** HyperDSC glass transitions for samples containing **a** 100%, **b** 10%, and **c** 1% amorphous maltitol. Heating rate was  $100\text{ }^{\circ}\text{C min}^{-1}$  and sample mass ca. 5 mg [18]

amorphous content the glass transition was easily seen such that the  $\Delta C_p$  value could be calculated (Fig. 3).

### StepScan DSC

The new stepwise DSC technique, StepScan DSC, is software for the characterization of thermal properties of materials [44–56]. The technique permits the separation of DSC data into thermodynamic (reversible) and kinetic (irreversible) components for better interpretation. StepScan produces a temperature program that consists of a series of short heat-hold steps [45–47]. After each step the heat flow is equilibrated until a given criterion is satisfied, and then the next step is started. The StepScan DSC

approach is only possible with the design of the power-compensated DSC, with its very low-mass sample and reference furnaces and rapid response time [47–49]. An empty-pan baseline should be run if an accurate  $C_p$  is needed [50].

The “Thermodynamic- $C_p$ ” data set reflects reversible (or fast) events, such as the sample’s heat capacity or glass transition. The kinetic or so-called “IsoK Baseline” data set reflects irreversible (or slow) processes taking place during the experiment, such as relaxation or crystallization. The temperature program used in StepScan DSC consists of alternate steps of heating with constant rate and isothermal holding. The reversible component is only observed in the heating part of the cycle and the irreversible one only in the isothermal part [46, 48, 51]. The duration of the isothermal part varies and the variation is controlled by the software which allows the sample to achieve a state close to the thermal equilibrium at each temperature step. No special mathematical operations, like Fourier transformation, are needed to obtain the results by the StepScan DSC technique [52]. The basic equation describing the heat flow response in a StepScan DSC experiment is given as:  $dQ/dt = C_p(dT/dt) + K(T,t)$ . In this equation,  $dQ/dt$  is the DSC heat flow,  $C_p$  is the sample’s specific heat capacity,  $dT/dt$  is the heating rate employed, and  $K(T,t)$  is the kinetic component [48, 51].

There are many measurement parameters in the StepScan DSC method. The three most important parameters are the length of the isothermal segment, the temperature jump between two subsequent isothermal segments, and the linear heating rate in the dynamic segments [46, 51]. There is also a criteria-parameter (= criteria to shorten the isotherm) which determines the length of the isotherms [45, 50]. A fine criterion requires a longer time but it allows higher accuracy in the measurement. The sensitivity of the measurement can be improved by using a high heating rate or a large sample. For calibration a relatively slow heating rate (e.g.,  $2\text{ }^{\circ}\text{C min}^{-1}$ ) is recommended because, in spite of a high partial heating rate in the dynamic segment, the overall heating rate is usually quite slow in StepScan measurements. Slow scan speeds in order to maintain steady state through the required number of oscillations result in longer experimental running times. StepScan DSC requires two separate scans, a blank scan and a sample scan, for any given set of experimental parameters, which results in a very time-consuming procedure.

In case the sample exhibits a glass transition with overlapping enthalpic relaxation, the Thermodynamic- $C_p$  signal would show the classic, stepwise change in the heat capacity, which simplifies the interpretation and makes the calculation of  $\Delta C_p$  much easier. The enthalpic relaxation event would then show up in the IsoK Baseline data set [47, 49, 50, 53]. This is illustrated in Fig. 4.

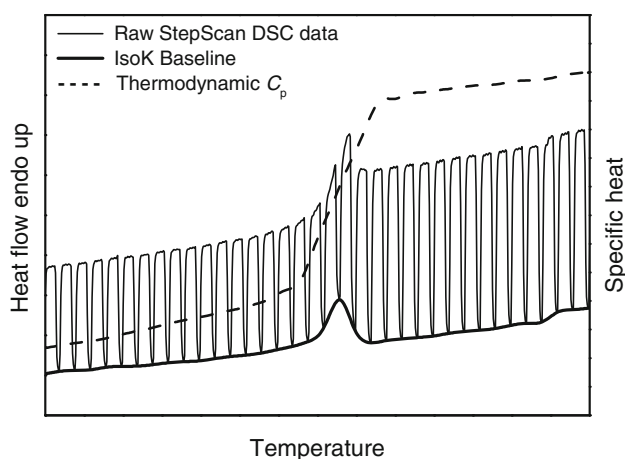


**Fig. 4** Typical StepScan DSC data for a glass transition: from the raw StepScan DSC data the IsoK Baseline curve and the thermodynamic- $C_p$  curve are calculated

Lehto et al. [8] determined the degree of amorphicity of lactose samples using StepScan DSC and compared the method to other methods that are widely used to quantify the degree of amorphicity (XRD, conventional DSC, IMC, SC, Raman spectrometry and GMS). The work revealed that the determination of  $\Delta C_p$  may be hampered in StepScan DSC by the fact that the baseline of the heat capacity curve is not always a straight line. It was found that the interpretation of the glass transition was very difficult when the change in specific heat is small (as in the case with a sample with 2% amorphicity). However, good correlation was found between the degree of amorphicity and  $\Delta C_p$ . Moreover, the StepScan DSC results were in good agreement with the results obtained with IMC, SC, Raman and GMS for the same samples [8].

Černošek et al. [52] evaluated the capability of the StepScan DSC technique to measure the glass transition of a model glass ( $As_2S_3$ ). The reversing (thermodynamic) part of the StepScan data about the glass transition region was found to remain completely unaffected by the choice of the experimental parameters such that both the  $\Delta C_p$  and  $T_g$  could be determined without influence of the thermal history experienced by the sample or the experimental conditions employed.

### Comparison of HyperDSC and StepScan DSC techniques

The sensitivity of the technique depends on the relative magnitude of the property change being measured. In DSC, detection of low concentrations of amorphous components is based on detection of changes in specific heat capacity associated with the glass transition. HyperDSC increases the sensitivity of DSC using a high heating rate. However,

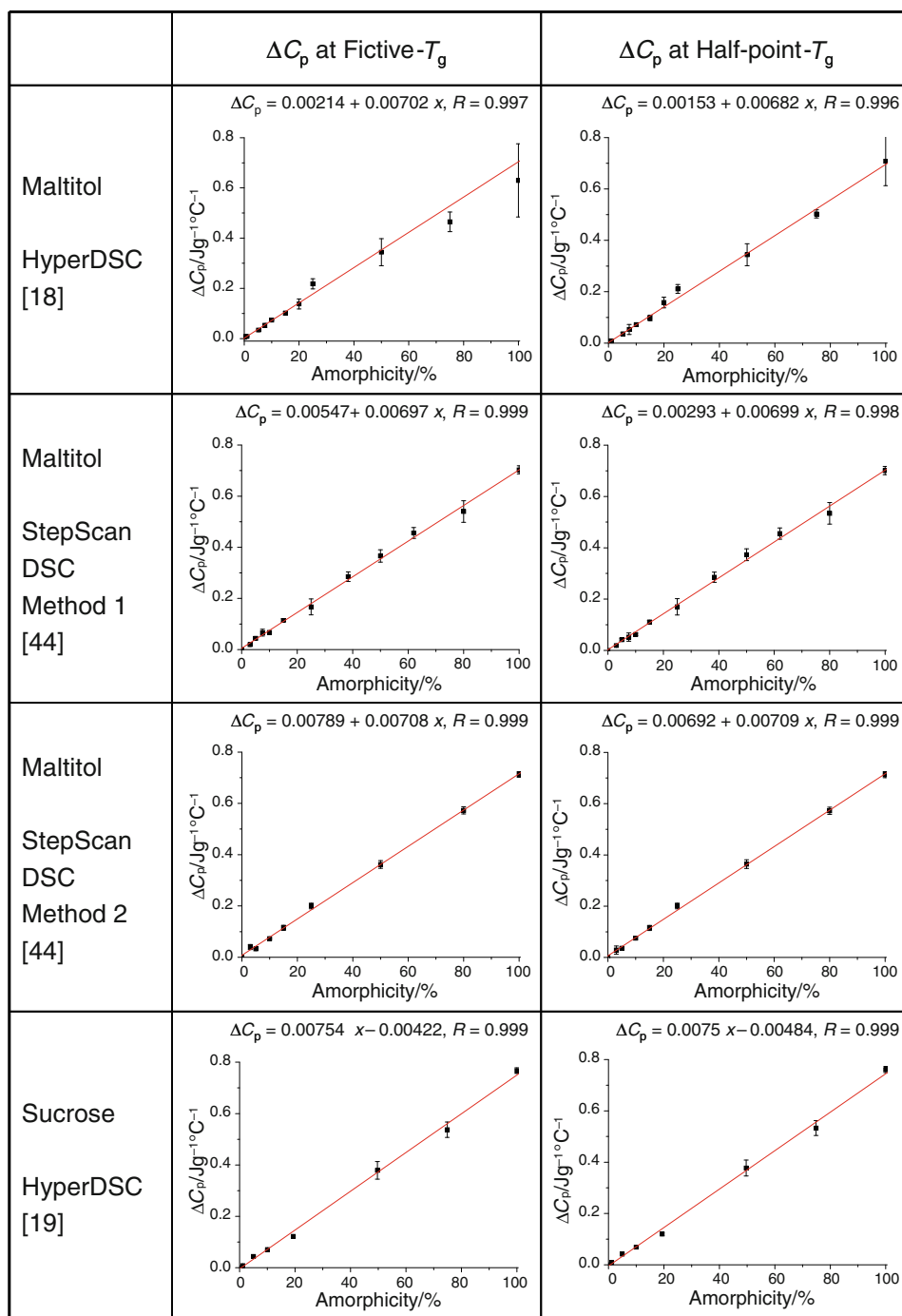
this approach also results in broadening and shifting of the glass transition, and does not always yield the desired sensitivity. Nevertheless, it should be emphasized that even though the value of  $T_g$  and also the heat capacity  $C_p$  will shift up with increasing heating rate, the magnitude of  $\Delta C_p$  does not change [52]. StepScan DSC, on the other hand, eliminates all baseline curvature and drift from the heat capacity signal and provides higher sensitivity for straightforward detection of weak glass transitions. However, in samples with extremely low concentrations of amorphous components, detecting the glass transitions may be a challenge and the calculation of the heat capacity change is impossible. Hence the suitability, selectivity, and limit of detection of each technique are sample-specific.

The capabilities of the two methods, HyperDSC and StepScan DSC, have been compared in quantification of low concentrations of amorphous components in sugar and sugar alcohol samples (maltitol and sucrose) [18, 19, 44]. In the StepScan measurements, two different heating rates were compared. For calibrations done at a heating rate of  $2\text{ }^\circ\text{C min}^{-1}$  the temperature program was: temperature increment  $2\text{ }^\circ\text{C}$ , heating rate  $2\text{ }^\circ\text{C min}^{-1}$ , isothermal period 1 min and criteria  $0.01\text{ mW}$  (= method 1). For calibrations done at a heating rate of  $10\text{ }^\circ\text{C min}^{-1}$  the temperature program was: temperature increment  $2\text{ }^\circ\text{C}$ , heating rate  $10\text{ }^\circ\text{C min}^{-1}$ , isothermal period 1 min and criteria  $0.0001\text{ mW}$  (= method 2). In the HyperDSC studies, the measurements were performed at a heating rate of  $100\text{ }^\circ\text{C min}^{-1}$ . The  $\Delta C_p$  values obtained for synthetic mixtures were used to calculate the average and standard deviation values and at least three parallel results were used for every lot. Moreover, the  $\Delta C_p$  values were calculated for both the fictive and the half-point glass transition temperatures for the sake of comparison, but no significant differences in the results were observed. The mean values of  $\Delta C_p$  about the glass transition region were plotted against the degree of amorphicity. The linear regression between  $\Delta C_p$  and the degree of amorphicity was obtained for both the techniques, as illustrated in Fig. 5.

Saklatvala et al. [17] compared the HyperDSC and TMDSC techniques using polyvinylpyrrolidone (PVP) samples. As a result of the higher scanning rate, the step change about the glass transition was much larger in the case of HyperDSC confirming that the faster scanning rate leads to an improvement in the sensitivity. At the same time, however, the transition was broader in HyperDSC. Modulated DSC enabled the separation of the enthalpic relaxation from the heat capacity change allowing for more straightforward detection of the glass transitions. However, detecting small glass transitions of amorphous components was a challenge.

The limit of detection (LOD) is defined as the analyte concentration giving a signal equal to the blank response

**Fig. 5** The average and standard deviation values for the specific heat change at glass transition temperature as function of amorphous content measured with HyperDSC and StepScan DSC for maltitol and sucrose samples [18, 19, 44]. The linear regression lines between  $\Delta C_p$  and amorphicity ( $x$ ) with  $R$ -values ( $R$  = correlation coefficient) are attached



plus three standard deviations of this value, whereas the limit of quantification (LOQ) is the analyte concentration giving a signal equal to the blank response plus 10 standard deviations of this value. From the regression lines the numerical information for constants  $b$ ,  $a$ ,  $s_a$ , and  $s_b$  can be obtained using the well-known equation of  $a = bx + y$  ( $s_a$  and  $s_b$  are standard deviations of  $a$  and  $b$ ). The LOD and LOQ values can be calculated using the equations  $X_L = 3s_a/b$  for LOD and  $X_L = 10s_a/b$  for LOQ [100]. Table 2 summarizes the LOD and LOQ values calculated

from data published for various lactose, maltitol, and sucrose samples. The values are appreciably low for both the HyperDSC and StepScan DSC techniques.

There are some characteristic differences in the HyperDSC and StepScan DSC methods when employed for the quantification of low amorphous contents. In HyperDSC the sensitivity is higher owing to the high heating rates used. The limit of quantification is determined by the measurement noise. Owing to the lower noise level in HyperDSC, lower LOD and LOQ values can be reached,

**Table 2** Calculated LOD and LOQ values from different references

| Sample   | Method       | Calculated from   | LOD/<br>% | LOQ/<br>% | References |
|----------|--------------|-------------------|-----------|-----------|------------|
| Maltitol | HyperDSC     | Fictive- $T_g$    | 0.31      | 1.04      | [18]       |
|          |              | Half-point- $T_g$ | 0.11      | 0.36      | [18]       |
| Sucrose  | HyperDSC     | Half-point- $T_g$ | 0.06      | 0.21      | [19]       |
| Lactose  | HyperDSC     | Half-point- $T_g$ | 0.57      | 1.89      | [15]       |
| Lactose  | HyperDSC     | Half-point- $T_g$ |           | <1.5      | [16]       |
| Maltitol | StepScan DSC | Method 1          |           |           |            |
|          |              | Fictive- $T_g$    | 0.24      | 0.81      | [44]       |
|          |              | Half-point- $T_g$ | 0.27      | 0.92      | [44]       |
| Maltitol | StepScan DSC | Method 2          |           |           |            |
|          |              | Fictive- $T_g$    | 0.18      | 0.61      | [44]       |
|          |              | Half-point- $T_g$ | 0.16      | 0.52      | [44]       |

and accordingly, smaller glass transitions can be detected. HyperDSC is also clearly faster than the StepScan DSC method. In some cases, however, distinguishing the glass transition from other thermal events (such as recrystallization and relaxation) has been found difficult in HyperDSC but can be readily achieved in StepScan DSC. The StepScan DSC measurements are more complicated to perform than the HyperDSC measurements. In the StepScan method, the proper choice of the various measurement parameters is important because they have a substantial effect on the results. Also the calibration method influences the results. However, the main advantage of the StepScan DSC method for quantification of an amorphous content is that the glass transition and relaxation peaks are separated to different curves such that the calculation of  $\Delta C_p$  becomes much easier.

## Conclusions

The change in the specific heat ( $\Delta C_p$ ) at the glass transition has been shown to be a good indicator for the degree of amorphicity in samples that are mostly crystalline. The two relatively new DSC techniques, HyperDSC and StepScan DSC, provide us with obvious benefits for the accurate  $\Delta C_p$  measurements. The former techniques improve in particular the sensitivity of the measurement whereas the main advantage of the StepScan DSC method is the easier data interpretation as it allows better distinguishment of the glass transition from other thermal events. With both the methods, experimental conditions can be found under which the degree of amorphicity linearly depends on  $\Delta C_p$  and low enough LOD and LOQ values are achieved. Hence, the two new DSC approaches should both be considered as highly potential techniques for quantifying low concentrations of amorphous phases in various crystalline matrices.

## References

- Hancock BC, Zografi G. Characteristics and significance of the amorphous state in pharmaceutical systems. *J Pharm Sci.* 1997;86:1–12.
- Cui Y. A material science perspective of pharmaceutical solids. *Int J Pharm.* 2007;339:3–18.
- Zhang GGZ, Law D, Schmitt EA, Qui Y. Phase transformation consideration during process development and manufacture of solid oral dosage forms. *Adv Drug Deliv Rev.* 2004;56:371–90.
- Craig DQM, Royall PG, Kett VL, Hopton ML. The relevance of the amorphous state to pharmaceutical dosage forms: glassy drugs and freeze dried systems. *Int J Pharm.* 1999;179:179–207.
- Saleki-Gerhardt A, Ahlneck C, Zografi G. Assessment of disorder in crystalline solids. *Int J Pharm.* 1994;101:237–47.
- Buckton G, Darcy P. Assessment of disorder in crystalline powders—a review of analytical techniques and their application. *Int J Pharm.* 1999;179:141–58.
- Giron D, Monnier S, Mutz M, Piechon P, Buser T, Stowasser F, Schulze K, Bellus M. Comparison of quantitative methods for analysis of polyphasic pharmaceuticals. *J Therm Anal Calorim.* 2007;89:729–43.
- Lehto V-P, Tenho M, Vähä-Heikkilä K, Harjunen P, Päällisaho M, Väilisaari J, Niemelä P, Järvinen K. The comparison of seven different methods to quantify the amorphous content of spray dried lactose. *Powder Technol.* 2006;167:85–93.
- Shah B, Kakumanu VK, Bansal AK. Analytical techniques for quantification of amorphous/crystalline phases in pharmaceutical solids. *J Pharm Sci.* 2006;95(8):1641–68.
- Nagapudi K, Jona J. Amorphous active pharmaceutical ingredients in preclinical studies: preparation, characterization and formulation. *Curr Bioact Compd.* 2008;4:213–24.
- Robinson P. HyperDSC, high speed DSC technique. Abstract Book of ESTAC8 2002, p. 101.
- Pijpers TF, Mathot VBF, Goderis B, Scherrenberg RL, van der Vegte EW. High-speed calorimetry for the study of kinetics of (de)vitrification, crystallization, and melting of macromolecules. *Macromolecules.* 2002;35:3601–13.
- Mathot VBF, Vanden Poel G, Pijpers TFJ. Improving and speeding up the characterization of substances, materials, and products: benefits and potentials of high-speed DSC. *Am Lab.* 2006;38(14):21–4.
- Pijpers MFJ, Mathot VBF. Optimization of instrument response and resolution of standard- and high-speed powder compensation DSC: benefits for the study crystallization, melting and thermal fractionation. *J Therm Anal Calorim.* 2008;93:319–27.
- Saunders M, Podlun K, Shergill S, Buckton G, Royall P. The potential of high speed DSC (Hyper-DSC) for the detection and quantification of small amounts of amorphous content in predominantly crystalline samples. *Int J Pharm.* 2004;274:35–40.
- Gabbott P, Clarke P, Mann T, Royall P, Shergill S. A high-sensitivity, high-speed DSC technique: measurement of amorphous lactose. *Am Lab.* 2003;35:17–18, 20, 22.
- Saklatvala RD, Saunders MH, Fitzpatrick S, Buckton G. A comparison of high speed differential scanning calorimetry (HyperDSC) and modulated differential scanning calorimetry to detect the glass transition of polyvinylpyrrolidone: the effect of water content and detection sensitivity in powder mixture (a model formulation). *J Drug Deliv Sci Technol.* 2005;15(4):257–60.
- Hurtta M, Pitkänen I. Quantification of low levels of amorphous content in maltitol. *Thermochim Acta.* 2004;419:19–29.
- Lappalainen M, Pitkänen I, Harjunen P. Quantification of low levels of amorphous content in sucrose by hyperDSC. *Int J Pharm.* 2006;307:150–5.



20. McGregor C, Saunders MH, Buckton G, Saklatvala RD. The use of high-speed differential scanning calorimetry (Hyper-DSC<sup>TM</sup>) to study the thermal properties of carbamazepine polymorphs. *Thermochim Acta*. 2004;417:231–7.
21. Ye P, Byron T. Characterization of D-Mannitol by thermal analysis, FTIR & Raman spectroscopy. *Am Lab*. 2008;40(14):24–7.
22. McGregor C, Bines E. The use of high-speed differential scanning calorimetry (HyperDSC) in the study of pharmaceutical polymorphs. *Int J Pharm*. 2008;350:48–52.
23. Gramaglia D, Conway BR, Kett VL, Malcolm RK, Batchelor HK. High speed DSC (hyper-DSC as a tool to measure the solubility of a drug within a solid or semi-solid matrix. *Int J Pharm*. 2005;301:1–5.
24. Buckton G, Adeniyi AA, Saunders M, Ambarkhane A. Hyper-DSC studies of amorphous polyvinylpyrrolidone in a model wet granulation system. *Int J Pharm*. 2006;312:61–5.
25. Vanden Poel G, Mathot VBF. High performance differential scanning calorimetry (HPer DSC): a powerful analytical tool for the study of the metastability of polymers. *Thermochim Acta*. 2007;461:107–21.
26. Vanden Poel G, Mathot VBF. High-speed/ high performance differential scanning calorimetry (HPer DSC): temperature calibration in the heating and cooling mode and minimization of thermal lag. *Thermochim Acta*. 2006;446:41–54.
27. Wunderlich B, Jin Y, Boller A. Mathematical description of differential scanning calorimetry based on periodic temperature modulation. *Thermochim Acta*. 1994;238:277–93.
28. Hu W, Wunderlich B. Data analysis without Fourier transformation for sawtooth-type temperature-modulated DSC. *J Therm Anal Calorim*. 2001;66:677–97.
29. Merzlyakov M, Schick C. Step response analysis in DSC—a fast way to generate heat capacity spectra. *Thermochim Acta*. 2001;380:5–12.
30. Bottom R. The role of modulated temperature differential scanning calorimetry in the characterization of a drug molecule exhibiting polymorphic and glass forming tendencies. *Int J Pharm*. 1999;192:47–53.
31. Salmerón Sánchez M, Gómez Ribelles JL, Hernández Sánchez FF, Mano JF. On the kinetics of melting and crystallization of poly(L-lactic acid) by TMDSC. *Thermochim Acta*. 2005;430:201–10.
32. Boller A, Schick C, Wunderlich B. Modulated differential scanning calorimetry in the glass transition region. *Thermochim Acta*. 1995;266:97–111.
33. Carpentier L, Desprez S, Descamps M. Crystallization and glass properties of pentitols: xylitol, adonitol, arabitols. *J Therm Anal Calorim*. 2003;73:577–86.
34. Verdonck E, Schaap K, Thomas LC. A discussion of the principles and applications of Modulated Temperature DSC (MTDSC). *Int J Pharm*. 1999;192:3–20.
35. Schawe JEK. Principles for the interpretation of modulated temperature DSC measurements: part 1: Glass transition. *Thermochim Acta*. 1995;261:183–94.
36. Hill VL, Craig DQM, Feely LC. The effects of experimental parameters and calibration on MTDSC data. *Int J Pharm*. 1999;192:21–32.
37. Boller A, Okazaki I, Wunderlich B. Modulated differential scanning calorimetry in the glass transition region: part III: Evaluation of polystyrene and poly(ethylene terephthalate). *Thermochim Acta*. 1996;284:1–19.
38. Schubnell M, Schawe JEK. Quantitative determination of the specific heat and the glass transition of moist samples by temperature modulated differential scanning calorimetry. *Int J Pharm*. 2001;217:173–81.
39. Craig DQM, Barsnes M, Royall PG, Kett VL. An evaluation of the use of modulated temperature DSC as a means of assessing the relaxation behaviour of amorphous lactose. *Pharm Res*. 2000;17(6):696–700.
40. Fraga I, Montserrat S, Hutchinson JM. TOPEM, a new temperature modulated DSC technique: application to the glass transition of polymers. *J Therm Anal Calorim*. 2007;87:119–24.
41. Chen K, Harris K, Vyazovkin S. Tacticity as a factor contributing to the thermal stability of polystyrene. *Macromol Chem Phys*. 2007;208:2525–32.
42. Fraga I, Montserrat S, Hutchinson JM. Vitrification during the isothermal cure of thermosets: part I. An investigation using TOPEM, a new temperature modulated technique. *J Therm Anal Calorim*. 2008;91:687–95.
43. Nor I, Sandu V, Ibanescu C, Hurduc N. Synthesis and characterization of star and brush grafted polysiloxanes, obtained by atom transfer radical polymerization. *e-Polymers*. 2008;138:1–15.
44. Lappalainen M, Pitkänen I. Quantification of amorphous content in maltitol by StepScan DSC. *J Therm Anal Calorim*. 2006;84:345–53.
45. Cassel B. A stepwise specific heat technique for dynamic DSC. *Am Lab*. 2000;32:23–6.
46. Pielichowski K, Flejtuch K, Pielichowski J. Step-scan alternating DSC study of melting and crystallization in poly(ethylene oxide). *Polymer*. 2004;45:1235–42.
47. Sichina WJ. Characterization of pharmaceuticals using thermal analysis. *Am Lab*. 2001;33:16–25.
48. Sichina WJ, Cassel RB. Enhanced characterization of materials using StepScan DSC. In: *Proceedings of the 28th NATAS conference on thermal analysis and applications*; 2000. p. 158–166.
49. Robinson P. Applications of StepScan modulated temperature DSC to plastic materials. *Med Plast*. 2001;15:114–7.
50. Cassel B, Scotto P, Sichina B. StepScan DSC. An alternative to conventional modulated techniques. In: *Proceedings of the 27th NATAS conference on thermal analysis and applications*; 1999. p. 33–36.
51. Sandor M, Bailey NA, Mathiowitz E. Characterization of polyandrydride microsphere degradation by DSC. *Polymer*. 2002;43:279–88.
52. Černošek Z, Holubová J, Černošková E. Capability of conventional differential scanning calorimetry (DSC), temperature modulated DSC (MDSC) and StepScan DSC for the glass transition phenomenon study. *Optoelectron Adv Mat*. 2007;1(6):277–80.
53. Chromčíková M, Holubová J, Liška M, Černošek Z, Černošková E. Modeling of the reversible part of StepScan DSC measurement of the glass transition. *Ceramics*. 2005;49:91–6.
54. Pielichowski K, Flejtuch K. Some comments on the melting and recrystallization of polyoxymethylene by high-speed and StepScan differential scanning calorimetry. *Polimery*. 2004;49:558–60.
55. Gunaratne LMWK, Shanks RA. Melting and thermal history of poly(hydroxybutyrate-co-hydroxyvalerate) using step-scan DSC. *Thermochim Acta*. 2005;430:183–90.
56. Holubová J, Černošek Z, Černošková E. The selenium based chalcogenide glasses with low content of As and Sb: DSC, StepScan DSC and Raman spectroscopy study. *J Non-Cryst Solids*. 2009;355:2050–3.
57. Byard SJ, Jackson SL, Smail A, Bauer M, Apperley DC. Studies on the crystallinity of a pharmaceutical development drug substance. *J Pharm Sci*. 2005;94(6):1321–35.
58. Chen X, Bates S, Morris KR. Quantifying amorphous content of lactose using parallel beam X-ray powder diffraction and whole pattern fitting. *J Pharm Biomed Anal*. 2001;26:63–72.

59. Fix I, Steffens K-J. Quantifying low amorphous or crystalline amounts of alpha-lactose-monohydrate using X-ray powder diffraction, near-infrared spectroscopy, and differential scanning calorimetry. *Drug Dev Ind Pharm.* 2004;30:513–23.
60. Gombás Á, Szabó-Révész P, Kata M, Regdon G Jr, Erös I. Quantitative determination of crystallinity of  $\alpha$ -lactose mono-hydrate by DSC. *J Therm Anal Calorim.* 2002;68:503–10.
61. Vemuri NM, Chrzan X, Cavatur R. Use of isothermal micro-calorimetry in pharmaceutical preformulation studies: part II. Amorphous phase quantification in a predominantly crystalline phase. *J Therm Anal Calorim.* 2004;78:55–62.
62. Bruni G, Milanese C, Bellazzi G, Berbenni V, Cofrancesco P, Marini A, Villa M. Quantification of drug amorphous fraction by DSC. *J Therm Anal Calorim.* 2007;89:761–6.
63. Lefort R, De Gussemme A, Willart J-F, Danène F, Descamps M. Solid-state NMR and DSC methods for quantifying the amorphous content in solid dosage forms: an application to ball-milling of trehalose. *Int J Pharm.* 2004;280:209–19.
64. Guinot S, Leveiller F. The use of MTDSC to assess the amorphous phase content of a micronized drug substance. *Int J Pharm.* 1999;192:63–75.
65. Saklatvala R, Royall PG, Craig DQM. The detection of amorphous material in a nominally crystalline drug using modulated temperature DSC—a case study. *Int J Pharm.* 1999;192:55–62.
66. Hogan SE, Buckton G. The application of near infrared spectroscopy and dynamic vapor sorption to quantify low amorphous contents of crystalline lactose. *Pharm Res.* 2001;18:112–6.
67. Mackin L, Zanon R, Park JM, Foster K, Opalenik H, Demonte M. Quantification of low levels (<10%) of amorphous content in micronized active batches using dynamic vapour sorption and isothermal microcalorimetry. *Int J Pharm.* 2002;231:227–36.
68. Ramos R, Gaisford S, Buckton G. Calorimetric determination of amorphous content in lactose: a note on the preparation of calibration curves. *Int J Pharm.* 2005;300:13–21.
69. Harjunen P, Lehto V-P, Koivisto M, Levonen E, Paronen P, Järvinen K. Determination of amorphous content of lactose samples by solution calorimetry. *Drug Dev Ind Pharm.* 2004;30:809–15.
70. Chadha R, Kashid N, Jain DVS. Characterization and quantification of amorphous content in some selected parenteral cephalosporins by calorimetric method. *J Therm Anal Calorim.* 2005;81:277–84.
71. Gustafsson C, Lennholm H, Iversen T, Nyström C. Comparison of solid-state NMR and isothermal microcalorimetry in the assessment of the amorphous component of lactose. *Int J Pharm.* 1998;174:243–52.
72. Royall PG, Huang C-Y, Jai Tang S-W, Duncan J, Van-deVelde G, Brown MB. The development of DMA for the detection of amorphous content in pharmaceutical powdered material. *Int J Pharm.* 2005;301:181–91.
73. Wu H-D, Wu S-C, Wu I-D, Chang F-C. Novel determination of the crystallinity of syndiotactic polystyrene using FTIR spectrum. *Polymer.* 2001;42:4719–25.
74. Taylor LS, Zografi G. The quantitative analysis of crystallinity using FT-Raman spectroscopy. *Pharm Res.* 1998;15:755–61.
75. Whiteside PT, Luk SY, Madden-Smith CE, Turner P, Patel N, George MW. Detection of low levels of amorphous lactose using H/D exchange and FT-Raman spectroscopy. *Pharm Res.* 2008;25(11):2650–6.
76. Venkatesh GM, Barnett ME, Owusu-Fordjour C, Galop M. Detection of low levels of the amorphous phase in crystalline pharmaceutical materials by thermally stimulated current spectrometry. *Pharm Res.* 2001;18:98–103.
77. Newell HE, Buckton G, Butler DA, Thielmann F, Williams DR. The use of inverse phase gas chromatography to measure the surface energy of crystalline, amorphous, and recently milled lactose. *Pharm Res.* 2001;18(5):662–6.
78. Ambarkhane AV, Pincott K, Buckton G. The use of inverse gas chromatography and gravimetric vapour sorption to study transitions in amorphous lactose. *Int J Pharm.* 2005;294:129–35.
79. Höhne GWH, Hemminger WF, Flammersheim H-J. Differential scanning calorimetry. 2nd ed. Berlin: Springer-Verlag; 2003.
80. Hilden LR, Morris KR. Physics of amorphous solids. *J Pharm Sci.* 2004;93(1):3–12.
81. Urbani R, Sussich F, Prejac S, Cesàro A. Enthalpy relaxation and glass transition behaviour of sucrose by static and dynamic DSC. *Thermochim Acta.* 1997;304/305:359–67.
82. Hancock BC, Shamblin SL, Zografi Z. Molecular mobility of amorphous pharmaceutical solids below their glass transition temperatures. *Pharm Res.* 1995;12:799–806.
83. Truong V, Bhandari BR, Howes T, Adhikari B. Physical aging of amorphous fructose. *J Food Sci.* 2002;67:3011–8.
84. Wungtanagorn R, Schmidt SJ. Thermodynamical properties and kinetics of the physical ageing of amorphous glucose, fructose, and their mixture. *J Therm Anal Calorim.* 2001;65:9–35.
85. Claudy P, Siniti M, El Hajri J. Thermodynamic study of the glass relaxation phenomena. DSC study of annealing maltitol glass. *J Therm Anal Calorim.* 2002;68:251–64.
86. Fan J, Angell A. Relaxational transitions and ergodicity breaking within the fluid state: the sugars fructose and galactose. *Thermochim Acta.* 1995;266:9–30.
87. Shamblin SL, Tang X, Chang L, Hancock BC, Pikal MJ. Characterization of the time scales of molecular motion in pharmaceutical important glasses. *J Phys Chem B.* 1999;103:4113–212.
88. Wunderlich B. Thermal analysis. San Diego: Academic Press Inc; 1990.
89. Roos Y. Phase transitions in foods. San Diego: Academic Press Inc; 1995.
90. Yu L. Amorphous pharmaceutical solids: preparation, characterization and stabilization. *Adv Drug Deliv Rev.* 2001;48:27–42.
91. Kerč J, Srčić S. Thermal analysis of glassy pharmaceuticals. *Thermochim Acta.* 1995;248:81–95.
92. Simatos D, Blond G, Roudaut G, Champion D, Perez J, Faivre AL. Influence of heating and cooling rates on the glass transition temperature and the fragility parameter of sorbitol and fructose as measured by DSC. *J Therm Anal.* 1996;47:1419–36.
93. Hancock BC, Zografi G. The relationship between the glass transition temperature and the water content of amorphous pharmaceutical solids. *Pharm Res.* 1994;11:471–7.
94. Roos Y, Karel M. Water and molecular weight effects on glass transitions in amorphous carbohydrates and carbohydrate solutions. *J Food Sci.* 1991;56:1676–81.
95. Noel TR, Paker R, Ring SG. Effect of molecular structure and water content on the dielectric relaxation behaviour of amorphous low molecular weight carbohydrates above their glass transition. *Carbohydr Res.* 2000;329:839–45.
96. Ahlneck C, Zografi G. The molecular basis of moisture effects on the physical and chemical stability of drugs in the solid state. *Int J Pharm.* 1990;62:87–95.
97. Byrn S, Pfeiffer R, Ganey M, Hoiberg C, Poochikian G. Pharmaceutical solids: a strategic approach to regulatory considerations. *Pharm Res.* 1995;12(7):945–54.
98. Perkin Elmer, Thermal Analysis Newsletter, Application Example PETAN-51.
99. Sebhatu T, Angberg M, Ahlneck C. Assessment of degree of disorder in crystalline solids by isothermal microcalorimetry. *Int J Pharm.* 1994;104:135–44.
100. Miller JC, Miller JN. Statistics for analytical chemistry. 3rd ed. Chichester: Ellis Horwood; 1993. p. 101–41.